JOC The Journal of Organic Chemistry

Article

pubs.acs.org/joc

Antioxidant Activity of *trans*-Resveratrol toward Hydroxyl and Hydroperoxyl Radicals: A Quantum Chemical and Computational Kinetics Study

Cristina Iuga,*[,†] J. Raúl Alvarez-Idaboy,[‡] and Nino Russo*[,§]

[†]Departamento de Ciencias Básicas, Universidad Autónoma Metropolitana-Azcapotzalco, 02200 México D.F., Mexico

[‡]Departamento de Física y Química Teórica, Facultad de Química, UNAM, 04510 México D.F., Mexico

[§]Dipartimento di Chimica, Università della Calabria, I-87036 Rende (CS), Italy

Supporting Information

ABSTRACT: In this work, we have carried out a systematic study of the antioxidant activity of *trans*-resveratrol toward hydroxyl (•OH) and hydroperoxyl (•OOH) radicals in aqueous simulated media using density functional quantum chemistry and computational kinetics methods. All possible mechanisms have been considered: hydrogen atom transfer (HAT), proton-coupled electron transfer (PCET), sequential electron proton transfer (SEPT), and radical adduct formation (RAF). Rate constants have been calculated using conventional transition state theory in conjunction with the Collins−Kimball theory. Branching ratios for the different paths contributing to the overall reaction, at 298 K, are reported. For the global reactivity of *trans*-resveratrol toward •OH radicals, in water at physiological pH, the main mechanism of reaction is proposed to be the sequential electron proton transfer (SEPT). However, we show that *trans*-resveratrol always reacts with •OH radicals at a rate that is diffusion-controlled, independent of the reaction pathway. This explains why *trans*-resveratrol is an excellent but very unselective •OH radical scavenger that provides antioxidant protection to the cell. Reaction between *trans*-resveratrol and the hydroperoxyl radical occurs only by phenolic hydrogen abstraction. The total rate coefficient is predicted to be 1.42×10^5 M^{-1} s^{-1}, which is much smaller than the ones for reactions of *trans*-resveratrol with •OH radicals, but still important. Since the •OOH half-life time is several orders larger than the one of the •OH radical, it should contribute significantly to *trans*-resveratrol oxidation in aqueous biological media. Thus, *trans*-resveratrol may act as an efficient •OOH, and also presumably •OOR, radical scavenger.

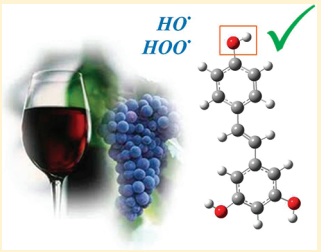

INTRODUCTION

trans-Resveratrol (*trans*-3,5,4′-trihydroxystilbene) is a triphenolic phytoalexin found in a variety of plant species,[1,2] such as grapevines, mulberries, peanuts, and the dried roots and stems of *Polygonium cuspidatum* (Japanese knotweed), and it is one of the most important polyphenols found in red wine. Its synthesis is triggered by plant stress conditions such as fungal infection, UV irradiation, and exposure to ozone or heavy metal ions.[1]

One of the most important biological activities of *trans*-resveratrol, and one that has been intensely investigated for the past few years, is its antioxidant behavior in biological systems.[3,4] It is associated with a surprising number of health benefits, most notably the mitigation of age-related diseases, including neurodegeneration, carcinogenesis, and atherosclerosis.[5]

The mitochondrial theory of aging, originally proposed by Harman in the early 1970s,[6] postulates that mitochondrial oxidative stress and the consequential free-radical reactions underlie aging. According to this theory, an increased production of ROS results in the accumulation of oxidative damage to proteins, lipids, and DNA, which is the primary causal factor of the aging process. There is clear evidence that aging in mammals is associated with mitochondrial oxidative stress in virtually every tissue studied, including blood vessels.[7−14] Recent studies suggest that longevity is associated with increased vascular resistance to high glucose-induced mitochondrial oxidative stress.[15] Recently, using animal models of diabetes mellitus, it has been shown that resveratrol could extend the life span by conferring vasoprotection.[16−20] Similar protective effects of resveratrol treatment were observed in aged mice.[12,16] Moreover, the consumption of Mediterranean-style diets, which are rich in resveratrol, is associated with a reduced risk of cardiovascular mortality in humans.[21,22]

In addition, *trans*-resveratrol has shown activity as an effective anticarcinogenic agent against several tumor cells, both in vitro and in vivo.[23,24] Data suggest that *trans*-resveratrol inhibits the proliferation of carcinogens through its interaction with the cytochrome P450 enzyme system.[24]

At the present time, lipid peroxidation is considered to be one of the basic mechanisms involved in reversible and irreversible cell and tissue damage. This chain-reaction process, which can be induced by a free-radical source, continually produces lipid peroxide radicals. In order to counterbalance the ROS, antioxidants act as biological bodyguards for essential

Received: January 30, 2012
Published: April 4, 2012

dx.doi.org/10.1021/jo3002134 | J. Org. Chem. 2012, 77, 3868−3877

molecules and combat oxidative stress by either neutralizing ROS or by repairing damage. *trans*-Resveratrol has the ability to break the chain-reaction process of lipid peroxidation by scavenging free radicals and forming phenoxy radicals that are stabilized by resonance. This results in the suppression of harmful self-propagating reactions induced by various free-radical sources.[25,26]

Many biologically relevant compounds exhibit second order $^{\bullet}$OH reaction rate constants of $10^{9}-10^{10}$ M^{-1} s^{-1}, which constitute essentially diffusion-limited reactivity.[27,28] It is generally believed that an indiscriminate attack on membranes, proteins, and other tissue constituents is a major reason for tissue damage during X-ray irradiation,[29] during exposure in vivo to OH-generating cellular toxins,[30] or in the presence of $^{\bullet}$OH-generating biochemical systems in vitro.[31] Previous studies have shown that $^{\bullet}$OH radicals are responsible for the ring-hydroxylation of a variety of aromatic compounds including phenol and substituted phenols such as tyrosine.[32−34]

The antioxidant activity of *trans*-resveratrol is related to its hydroxyl (OH) groups, which can scavenge free radicals produced in vivo.[35] Experimental data demonstrate that if the OH groups are eliminated or replaced by OCH_3, the molecule loses its activity. In addition, as demonstrated in experimental studies on the reactions of *trans*-resveratrol and its derivatives, the 4′-hydroxyl group is the most reactive one.[36−39]

Parallel to experimental studies, the antioxidative activity of *trans*-resveratrol has also been studied theoretically. On the basis of DFT computations of the OH reactions of *trans*-resveratrol and its hydroxylated derivatives in the gas phase, Queiroz et al.[40] have shown that it is related to the stabilization energy of the formed free radicals, which in turn depends on their π-electron system and on the number of possible resonance structures.

Bond dissociation energies (BDE) and ionization potentials (AIP) for *trans*-resveratrol and other phenolic antioxidants have been determined both in the gas phase[44] and in solution.[41,42] They found that it reacts with free radicals preferentially by a hydrogen-transfer mechanism (HAT) rather than by an electron transfer. However, Caruso et al.[43] proved that proton transfer is the dominant mechanism of the reaction of free radicals with various antioxidants and that the para 4′-OH group is more acidic than the other hydroxyl groups; this observation correlates with its scavenging free-radical ability. Unfortunately, in this study, the influence of the solvent was not taken into consideration.

A theoretical study of the antioxidant activity of *trans*-resveratrol was also performed by Cao et al.[44] based on a spin density analysis and single electron distribution. The authors show that the strong antioxidant action is due to the formation of radicals with a semiquinone structure, in which the unpaired electron is mainly localized on the O-atoms at the *para* and *ortho* positions. In agreement with other authors, they found that the 4′-hydroxyl group is the preferred reaction site, although the other hydroxyl groups and the double bond contribute to the free-radical scavenging ability. However, the computations reported in this work were only performed in the gas phase, and the results may not be valid in a cellular environment. Furthermore, the gas- and liquid-phase acidity of *trans*-resveratrol have been determined at DFT level of theory.[45] No kinetic data were reported.

There are numerous types of free radicals that can be formed within the body. The hydroxyl radical is the most electrophilic[46] and most reactive of the oxygen-centered radicals, with a half-life of $\sim 10^{-9}$ s.[47] Compared with the $^{\bullet}$OH radicals, the hydroperoxyl ($^{\bullet}$OOH) radical is a relatively slow-reacting species with half-lives of the order of seconds,[48] capable of diffusing to remote cellular locations.[49] The $^{\bullet}$OOH radical is the protonated form of the superoxide radical anion, $O_2^{\bullet-}$.[50] Since the protonation/deprotonation equilibrium exhibits a pK_a of 4.8, only about 0.3% of any superoxide present in a typical cell is in the protonated form. However, $O_2^{\bullet-}$ is not a very reactive species, so the chemistry of superoxide in living systems is probably dominated by $^{\bullet}$OOH radical reactions.[47] Moreover, the behavior of $^{\bullet}$OOH is probably similar to the one of larger peroxyl radicals, $RO_2^{\bullet}$, which are abundant in biological systems. Thus, the studying of $^{\bullet}$OOH may yield insight on the reactions of other important radicals.

In order to help understand the global reactivity of *trans*-resveratrol toward free radicals in biological media, we have carried out a systematic study of the reactivity of *trans*-resveratrol toward hydroxyl ($^{\bullet}$OH) and hydroperoxyl ($^{\bullet}$OOH) radicals in aqueous simulated media, using density functional quantum chemistry and computational kinetics methods. All possible mechanisms have been considered: hydrogen atom transfer (HAT), proton-coupled electron transfer (PCET), sequential electron proton transfer (SEPT), and radical adduct formation (RAF). Rate constants have been calculated using conventional transition state theory in conjunction with the Collins−Kimball theory. Branching ratios for the different paths contributing to the overall reaction, at 298 K, are reported.

COMPUTATIONAL METHODOLOGY

All electronic calculations were performed with the Gaussian 09 system of programs.[51] Geometry optimizations and frequency calculations have been carried out using the M05-2X functional[52] in conjunction with the 6-311++G(d,p) basis set. The M05-2X functional has been recommended for kinetic calculations,[52] and it has been successfully used by independent authors for that purpose.[53] Unrestricted calculations were used for open-shell systems. Local minima and transition states were identified by the number of imaginary frequencies: local minima have only real frequencies, while transition states are identified by the presence of a single imaginary frequency that corresponds to the expected motion along the reaction coordinate. Relative energies are calculated with respect to the sum of the separated reactants. Zero-point energies (ZPE) and thermal corrections to the energy (TCE) at 298 K are included in the determination of energy barriers.

We have assumed that reactions take place according to the complex two-step typical mechanism of radical−molecule reactions, in which the initial step leads to the formation of a prereactive complex (RC) that is in equilibrium with the reactants (R), and the second step is the irreversible formation of the products.[54]

Solvent effects are introduced using the SMD continuum model.[55] Although the dielectric constant of cellular environments is somewhat reduced by the presence of macromolecules and cosolvents, it is clear that water is, by far, their major component. Thus, in this work, water has been used as the cellular solvent.

Solvent cage effects have been included according to the corrections proposed by Okuno[56] and taking into account the free volume theory.[57] These corrections are in good agreement with those independently obtained by Ardura et al.[58] In this work, the expression used to correct the Gibbs free energy is

$$\Delta G_{sol}^{FV} \cong \Delta G_{sol}^{0} - RT\{\ln[n10^{(2n-2)}] - (n-1)\} \quad (1)$$

where n represents the molecularity of the reaction. According to expression 1, the cage effects in solution cause ΔG to decrease by 2.54 kcal/mol for bimolecular reactions at 298.15 K. The packing effects of the solvent reduce the entropy loss associated with any chemical reactions with molecularity equal to, or larger than, 2.

dx.doi.org/10.1021/jo3002134 | J. Org. Chem. 2012, 77, 3868−3877

Rate constants have been calculated using conventional transition state theory (TST)[59−61] as implemented in TheRate program[62] at the Computational Science and Engineering Online website (www.cseo.net)[63] and 1 M standard state as

$$k = \sigma\kappa\frac{k_B T}{h}e^{-(\Delta G^{\ddagger})/RT} \quad (2)$$

where k_B and h are the Boltzman and Planck constants; $\Delta G^{\ddagger}$ is the Gibbs free energy of activation; σ represents the reaction path degeneracy, accounting for the number of equivalent reaction paths; and κ accounts for tunneling corrections. The latter are defined as the Boltzman average of the ratio between the quantum and classical probabilities, and they were calculated using the zero-curvature tunneling (ZCT) method using an Eckart barrier.[64,65] The energy values, partition functions, and thermodynamic data were taken from the quantum-mechanical calculations.

Direct reaction branching ratios (Γ), are computed as

$$\Gamma_{path} = \frac{k_{path}}{k^{overall}} \times 100 \quad (3)$$

For the mechanisms involving single-electron transfers (SET), the Marcus theory was used.[66−68] Within this transition-state formalism, the SET activation barrier ($\Delta G^{\ddagger}_{SET}$) is defined in terms of the free energy of reaction (ΔG^{0}_{SET}) and the nuclear reorganization energy (λ):

$$\Delta G^{\ddagger}_{SET} = \frac{\lambda}{4}\left(1 + \frac{\Delta G^{0}_{SET}}{\lambda}\right)^2 \quad (4)$$

Reorganization energy (λ) has been calculated as

$$\lambda = \Delta E_{SET} - \Delta G^{0}_{SET} \quad (5)$$

where ΔE_{SET} has been calculated as the nonadiabatic energy difference between reactants and vertical products. This approach is similar to the one previously used by Nelsen and co-workers[69,70] for a large set of self-exchange reactions.

Some of the calculated rate constants (k) values are close to (or are, in fact) diffusion-limit rate constants. Accordingly, the apparent rate constant (k_{app}) cannot be directly obtained from TST calculations. In the present work, the Collins−Kimball theory is used for that purpose[71]

$$k_{app} = \frac{k_D k}{k_D + k} \quad (6)$$

where k is the thermal rate constant, obtained from TST calculations, and k_D is the steady-state Smoluchowski[72] rate constant for an irreversible bimolecular diffusion-controlled reaction

$$k_D = 4\pi R D_{AB} N_A \quad (7)$$

where R denotes the reaction distance, N_A is the Avogadro number, and D_{AB} is the mutual diffusion coefficient of the reactants A (free radical) and B (resveratrol). D_{AB} has been calculated from D_A and D_B according to ref 73, and D_A and D_B have been estimated from the Stokes−Einstein approach[74]

$$D = \frac{k_B T}{6\pi\eta a} \quad (8)$$

where k_B is the Boltzmann constant, T is the temperature, η denotes the viscosity of the solvent (in our case water, $\eta = 8.91 \times 10^{-4}$ Pa s), and a is the radius of the solute.

A recent work on the reaction between $OOCH_3$ radical and quercetin[75] demonstrated that kinetic data coming from TST and CVT computations are very similar. The computational methodology used in this manuscript has been successfully employed for similar studies[76,77]

RESULTS AND DISCUSSION

The optimized structure of *trans*-resveratrol is shown in Figure 1, where we have indicated the atomic numbering scheme. The

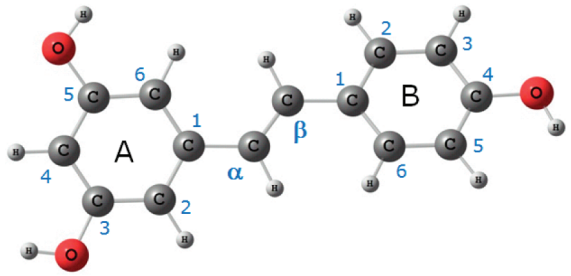

Figure 1. Optimized structure of *trans*-resveratrol in water.

results show that *trans*-resveratrol has an approximately planar structure in which the dihedral angle between the two benzene rings is about 0.34° (Figure 1).

In an aqueous environment, a large number of possible reactions can occur, in principle, between *trans*-resveratrol and free radicals. They can be grouped into two basic types of mechanisms: (i) hydrogen atom abstraction and (ii) radical addition (radical adduct formation, RAF). Hydrogen atom abstraction can occur according to three different mechanisms: sequential electron−proton transfer (SEPT), proton-coupled electron transfer (PCET), and direct hydrogen atom transfer (HAT). In this work, we have considered the three phenolic H-abstraction paths (from positions 3A, 5A, and 4B), with the subsequent formation of a water molecule and the corresponding radical as well as all possible addition channels (addition to the >C═C< moiety and addition to the A and B aromatic rings).

All these mechanisms could in principle occur in parallel, although at different rates. One of the objectives of the present work is to determine which mechanism has the faster rate constant, in the reactions of *trans*-resveratrol with both hydroxyl ($^{\bullet}OH$) and hydroperoxyl ($^{\bullet}OOH$) free radicals.

$^{\bullet}$OH-Initiated Oxidation of *trans*-Resveratrol. Once $^{\bullet}OH$ radicals are formed in a biological environment, they react instantaneously at essentially diffusion-controlled rates, indicating very low barriers and large exothermicity. The reaction products can be either OH-adduct radicals, as in the case of addition to the various nucleotide bases, or net dehydrogenation radicals produced by water elimination.

In order to study the reactivity of *trans*-resveratrol toward $^{\bullet}OH$ radicals in aqueous media, we have considered all hydrogen atom transfer (HAT), proton-coupled electron transfer (PCET), sequential electron proton transfer (SEPT), and radical adduct formation (RAF) pathways, according to the following reactions:

$$RV + {}^{\bullet}OH \rightarrow RV(-H)^{\bullet} + H_2O \qquad (HAT/PCET)$$

$$RV + {}^{\bullet}OH \rightarrow RV^{+\bullet} + OH^{-} \leftrightarrow RV(-H)^{\bullet} + H_2O \quad (SEPT)$$

$$RV + {}^{\bullet}OH \rightarrow RV(OH)^{\bullet} \qquad (RAF)$$

We have recently shown that, for dopamine,[75] the $^{\bullet}OH$ hydrogen abstraction is barrierless and it occurs preferentially via PCET; i.e., the proton transfer is coupled to an electron transfer. This seems to be the general mechanism for phenols

dx.doi.org/10.1021/jo3002134 | J. Org. Chem. 2012, 77, 3868−3877

that are capable of reacting by single electron transfer (SET), and it is the case, also, for *trans*-resveratrol. Using partial optimization with constrained O---H---OH bonds, we have obtained a saddle-point structures with an imaginary frequency. However, a subsequent unfreezing of the two distances involved, followed by optimization to a saddle point, produces an increase of the H---OH distance, and a corresponding decrease of the imaginary frequency and of the gradient, leading to the separated reactants. A relaxed scan, obtained by decreasing the H---H distance, produces an equivalent result: in this case, the energy decreases until the H atom is completely transferred. This result means that the reaction is strictly diffusion-controlled; i.e., every encounter results in a reaction. At this point, it is important to mention that when the $^{\bullet}$OH radical is relatively close to a phenolic H, the charge on the $^{\bullet}$OH radical oxygen atom is approximately −1.27 electrons, which is consistent with a PCET mechanism rather that a HAT mechanism. Also, charge separation between the phenolic group and the $^{\bullet}$OH radical is clearly favored by the polar solvent.

The dominant structure of the corresponding formed radicals is a semiquinone structure which favors their stability, and the unpaired electron is mainly located on the O-atom at the ortho and para positions. The formed radicals present large exergonicity (−31.43, −31.97, and −37.84 kcal/mol, resvectively) relative to reactants. The 4B-hydroxyl group is probably the most reactive site because of the resonance effects that occur between the two aromatic rings. This hydroxyl group is located in a para position with respect to the styrene moiety, which contains a benzene ring substituted by two other OH groups in meta positions. The effect of the latter is to donate electron pairs that can be transmitted, via the stilbene bridge, all the way to the para position on the second benzene ring. The relevance of this type of conjugation in electron transfer processes has been reported previously.[78]

The optimized structures of the product complexes are shown in Figure 2. In these structures, the water molecule forms an hydrogen bond with the corresponding radical.

Although phenolic H-abstractions are PCET mechanisms, the corresponding individual rate constants are diffusion-controlled and equal to the diffusion rate constant 1.98×10^9 M^{-1} s^{-1} at 298 K. Thus, the total PCET rate constant, calculated as the sum of the individual rates of the PCET phenolic H-abstraction, is 5.94×10^9 M^{-1} s^{-1} at 298 K.

The sequential electron−proton transfer (SEPT) process also occurs in polar solutions, since the polar environment is expected to promote solvation of the intermediate ionic species formed, thus favoring electron transfer. In this mechanism, the radical cation is first formed, followed by rapid and reversible deprotonation.

It is well-known that phenolic compounds are oxidized to quinones via semiquinones formation in SEPT processes that eliminate protons from the phenolic groups.[79] In the SEPT mechanism, the sequential transfer can take place in two different ways: (i) a single-electron transfer (SET) process followed by deprotonation of the formed radical cation or (ii) a deprotonation followed by a SET process from the formed anion. Since the polar environment is expected to promote solvation of the intermediate ionic species formed, the electron-transfer process is expected to be favored.

Because the three hydroxyls of *trans*-resveratrol show dissimilar activity in scavenging free radicals, three H-atom-transfer reactions between an $^{\bullet}$OH radical and hydroxyl groups at different positions were studied. The proposed two-step SEPT mechanism for *trans*-resveratrol oxidation is represented in Scheme 1. In the SET process, a radical cation ($RV^{\bullet+}$) is obtained; the phenolic groups of the radical cation ($RV^{\bullet+}$) obtained via SET is relatively acidic: the calculated pK_a for the 3A, 5A, and 4B sites are −0.03, −0.43, and −4.73, respectively. In the second step, in principle, there are three possible pathways, corresponding to the deprotonation at the 3A, 5A, and 4B phenolic groups. The final products are the same as the ones obtained via HAT direct H-abstractions, and therefore, the overall ΔG values are the same. However, the Gibbs free energy values of the second step are calculated relative to the $RV^{\bullet+}$ intermediate obtained in the SET process, and we find that the

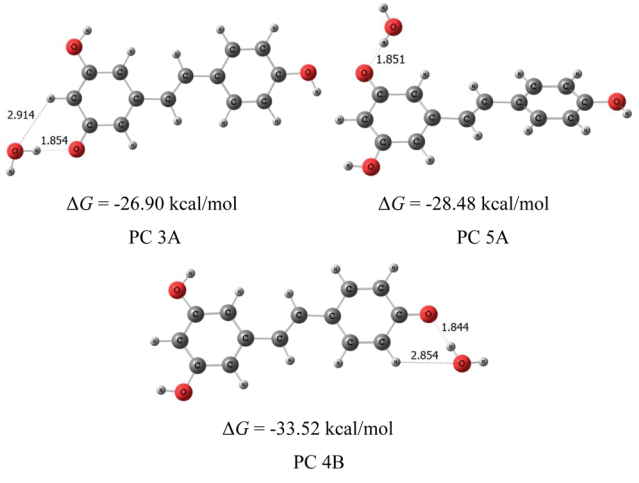

Figure 2. Optimized structures of the HAT/PCET product complexes.

Scheme 1. SEPT Mechanism for *trans*-Resveratrol Oxidation by $^{\bullet}$OH radicals

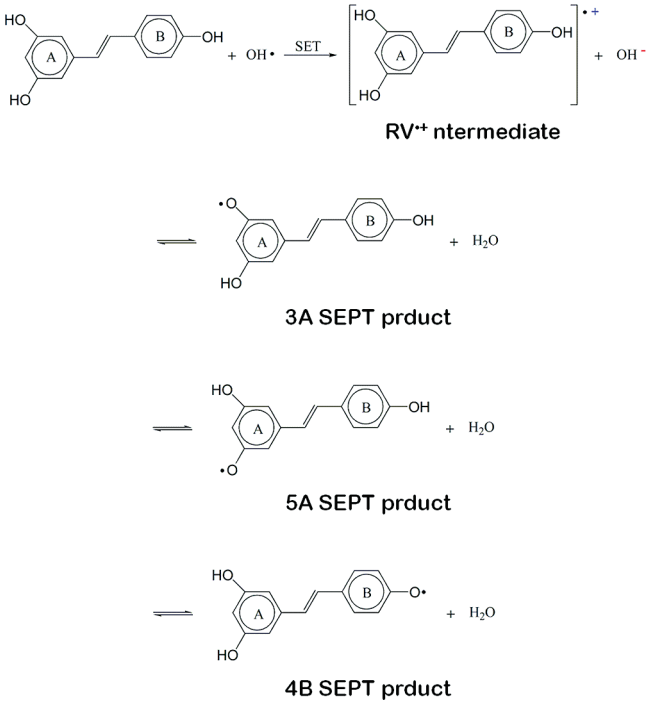

dx.doi.org/10.1021/jo3002134 | J. Org. Chem. 2012, 77, 3868−3877

most exergonic pathway is 4B (ΔG = −10.60 kcal/mol), while 3A and 5A positions are almost equivalent, and their ΔG are very close (−4.20 and −4.74 kcal/mol, respectively). Therefore, the 4B radical is expected to be the major product in the SEPT reaction.

At physiological pH, an equilibrium exists between the radical cation and the radical deprotonated form ($RV^{\bullet}$), which is identical to the HAT/PCET product. Therefore, the radicals obtained via H-abstraction from the phenolic groups are in equilibrium with the radicals cations ($RV^{\bullet+}$) obtained via the SET mechanism. The equilibrium between the cation ($RV^{\bullet+}$) and neutral *trans*-resveratrol depends on pH. However, because of the small OH^- anion concentration, at neutral pH, ($RV^{\bullet+}$) is favored.

The reorganization energy (λ), the Gibbs activation free energy ($\Delta G^{\ddagger}$), the SET rate constant (k^{SET}), and the apparent rate constant (k_{app}^{SET}) of the initial single-electron transfer between *trans*-resveratrol and an $^{\bullet}OH$ radical are reported in Table 1. ΔE^{SET} has been calculated as the nonadiabatic energy

Table 1. Reorganization Energy (λ, kcal/mol), Gibbs Free Energy of Activation ($\Delta G^{\ddagger}$, kcal/mol), Diffusion Rate Constant (k_D, M^{-1} s^{-1}), SET Rate Constant (k^{SET}, M^{-1} s^{-1}), and Apparent Rate Constant (k_{app}^{SET}, M^{-1} s^{-1}) in the $^{\bullet}OH$ Radical SET Mechanism

λ	$\Delta G^{\ddagger}$	ΔG	k_D	k^{SET}	k_{app}^{SET}
10.08	0.33	−6.41	7.95×10^9	8.71×10^{13}	7.95×10^9

difference between reactants and vertical products, i.e., $RV^{\bullet+}$ and OH^- at the neutral RV and $^{\bullet}OH$ geometries. $\Delta G^{\ddagger}$ has been evaluated using the Marcus theory. Since the subsequent proton transfer is known to be very fast, the SET and SEPT rate constants are the same.

Our computations show that the SEPT process in Scheme 1 is diffusion-controlled. The diffusion rate constant k_D has been calculated according to eq 6 and is also included in Table 1 for comparison. The products obtained in the SEPT reaction are the same as in the PCET channels.

The radical adduct formation (RAF) process may also occur, with $^{\bullet}OH$ addition either to the >C═C< moiety (at positions C_α and C_β), or to the A and B aromatic rings. Optimized structures for transition states (TS) and adducts in the OH-addition reactions to the >C═C< moiety and to the A and B aromatic rings are presented in Figures 3, 4 and 5, respectively, and relative energies (including ZPE) and Gibbs free energies (including TCE at 298 K), calculated at the M05-2X/6-311++G** level, are reported in Table 2. The TST thermal (k^{RAF}) and diffusion-corrected apparent (k_{app}^{RAF}) rate constants for the different OH-addition channels, calculated at 298 K, are also reported in Table 2.

All additions occur in a similar way and destroy the aromaticity of the ring. The $^{\bullet}OH$ radical oxygen atom approaches either a >C═C< carbon atom or one of the aromatic rings. The transition vector in the transition-state structures corresponds to the vertical movement of the OH group in the direction of the carbon site. The H atom or −OH phenolic groups attached to the carbon atom fold back slightly to accommodate the incoming $^{\bullet}OH$ radical. Cartesian coordinates of all the RAF transition structures are given in Table S1 of the Supporting Information.

All of the RAF pathways were found to be exergonic (ΔG < 0). The largest exergonicity corresponds to the Cα and Cβ

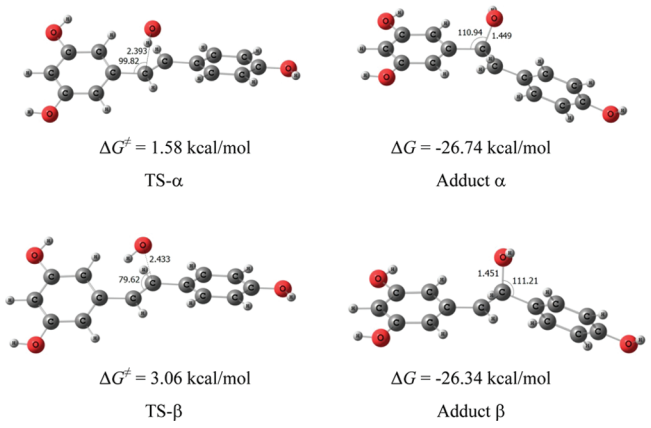

Figure 3. Transition structures (TS) and adducts in the $^{\bullet}OH$ addition to the >C═C< moiety.

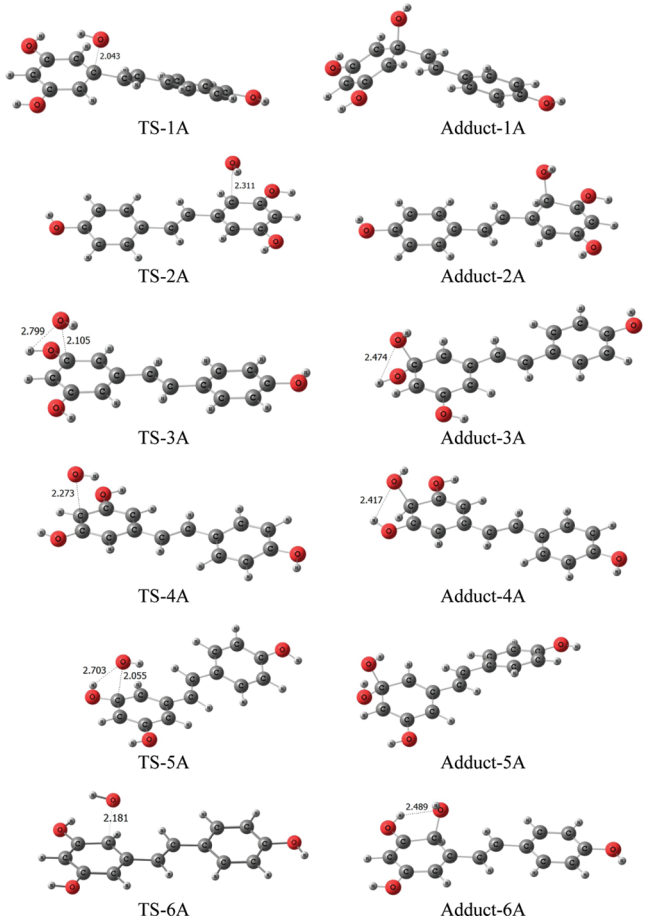

Figure 4. Transition structures and adducts in the OH-addition channels to the A aromatic ring.

addition pathways: −26.74 and −26.34 kcal/mol, respectively. Moreover, almost all $^{\bullet}OH$-addition channels are diffusion-controlled, except to the 3A and 5A positions, which are less favored. The diffusion rate constant in water for *trans*-resveratrol is 1.98×10^9 M^{-1} s^{-1} at 298 K. Thus, a mixture of adducts are expected to occur under equilibrium conditions. The total rate constant for the RAF OH-addition pathways is 2.26×10^{10} M^{-1} s^{-1} at 298 K.

dx.doi.org/10.1021/jo3002134 | J. Org. Chem. 2012, 77, 3868−3877

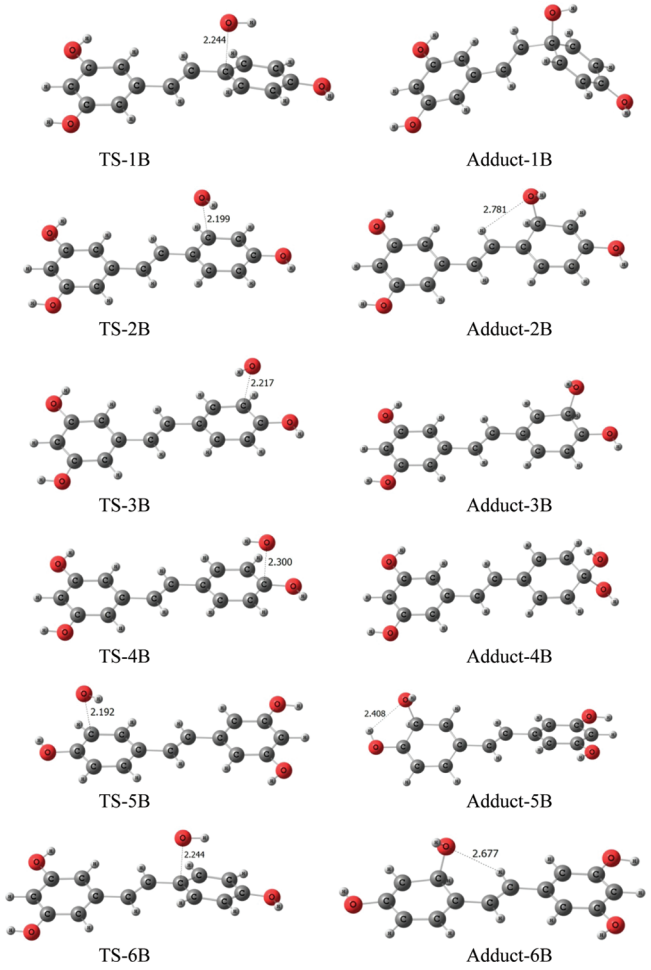

Figure 5. Transition structures and adducts in the $^{\bullet}$OH addition channels to the B aromatic ring.

The overall rate constant, which measures the rate of $^{\bullet}$OH disappearance, has been estimated by summing up the total rate coefficients calculated for all the competing mechanisms:

$$k^{\bullet OH}(\text{water}) = k_{app}^{PCET} + k_{app}^{SCET} + k_{app}^{RAF}$$

Each term includes all channels of the same type. Thus, the calculated overall diffusion-corrected apparent rate constant in *trans*-resveratrol + $^{\bullet}$OH in aqueous solution is equal to 3.65×10^{10} M^{-1} s^{-1}. Direct reaction branching ratios (Γ), are computed according to eq 3 and are reported in Table 3.

Table 3. Diffusion-Corrected Apparent Rate Constants, in M^{-1} s^{-1}, and Direct Branching Ratios (Γ) at 298 K, in the *trans*-Resveratrol Oxidation by $^{\bullet}$OH Radicals in Water

path	k_{app}	Γ (%)
PCET	5.94×10^9	~16.3
SEPT	7.95×10^9	~21.8
RAF	2.26×10^{10}	~61.9

The branching ratios of the viable reaction channels, which represent the percent of their contribution to the overall reaction, show that the OH scavenging activity of *trans*-resveratrol takes place predominantly by a RAF mechanism (~61.9%). However, the rate constant of the SEPT reaction (7.95×10^9 M^{-1} s^{-1}) is larger than any individual RAF rate constant. In addition, it is interesting to point out that, because single electron transfer can occur when the reactants are at much larger distances than in either direct H atom transfer (HAT) or $^{\bullet}$OH-addition, the corresponding calculated diffusion limit for SET is larger.

$^{\bullet}$OOH-Initiated Oxidation of *trans*-Resveratrol. As in the previous section, in order to study the reactivity of *trans*-resveratrol toward $^{\bullet}$OOH radicals, we have considered all H-abstraction, proton-coupled electron transfer (PCET), sequential electron proton transfer (SEPT), and radical adduct formation (RAF) pathways, according to:

$$RV + {}^{\bullet}OOH \rightarrow RV(-H)^{\bullet} + H_2O_2 \qquad \text{(HAT/PCET)}$$

$$RV + {}^{\bullet}OOH \rightarrow RV^{+\bullet} + OOH^{-} \leftrightarrow RV(-H)^{\bullet} + H_2O_2 \qquad \text{(SEPT)}$$

$$RV + {}^{\bullet}OOH \rightarrow RV(OOH)^{\bullet} \qquad \text{(RAF)}$$

The transition structures corresponding to the phenolic H-abstraction pathways are shown in Figure 6. The terminal oxygen atom of the $^{\bullet}$OOH radical approaches the hydrogen

Table 2. Relative Energies (Including ZPE) and Relative Gibbs Free Energies (Including TCE at 298 K), in kcal mol^{-1}, and TST Thermal (k^{RAF}, M^{-1} s^{-1}) and Diffusion-Corrected Apparent (k_{app}^{RAF}, M^{-1} s^{-1}) Rate Constants Calculated at 298 K, in the RAF $^{\bullet}$OH Addition Pathways

path	$\Delta E^{\ddagger}$	ΔE	$\Delta G^{\ddagger}$	ΔG	k^{RAF}	k_{app}^{RAF}
Cα	−3.54	−33.27	1.58	−26.74	2.11×10^{13}	1.98×10^9
Cβ	−2.68	−32.62	3.06	−26.34	1.74×10^{12}	1.98×10^9
C1A	3.66	−10.38	9.38	−3.82	4.04×10^7	3.96×10^7
C2A	−3.77	−21.80	1.86	−15.01	1.32×10^{13}	1.98×10^9
C3A	2.04	−16.64	8.44	−10.14	1.98×10^8	1.80×10^8
C4A	−3.31	−24.47	3.01	−17.66	1.89×10^{12}	1.98×10^9
C5A	0.63	−16.88	7.06	−10.57	2.03×10^9	1.00×10^9
C6A	−4.59	−23.10	0.90	−16.05	6.65×10^{13}	1.98×10^9
C1B	−0.76	−13.71	5.39	−6.90	3.40×10^{10}	1.87×10^9
C2B	−0.63	−19.08	5.18	−12.52	4.85×10^{10}	1.90×10^9
C3B	−1.16	−17.06	4.97	−10.56	6.91×10^{10}	1.92×10^9
C4B	−1.10	−25.28	4.71	−18.73	1.07×10^{11}	1.94×10^9
C5B	−0.99	−16.54	5.05	−9.94	6.04×10^{10}	1.92×10^9
C6B	−1.16	−21.70	4.71	−14.79	5.33×10^{10}	1.92×10^9

dx.doi.org/10.1021/jo3002134 | J. Org. Chem. 2012, 77, 3868−3877

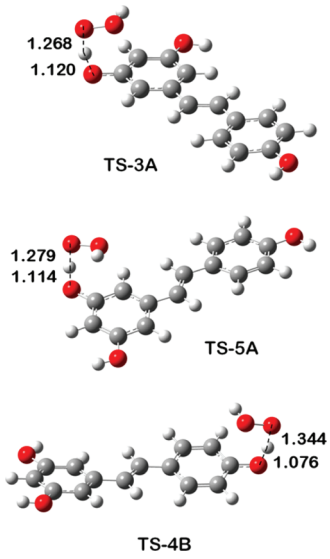

Figure 6. Transition structures (TS) in the phenolic H-abstraction by $^{\bullet}$OOH radicals.

atom to be abstracted, as the energy increases to a maximum along the reaction path.

In the transition-state structures, the $^{\bullet}$OOH radical is located approximately perpendicular to the *trans*-resveratrol molecular plane. The vibrational mode corresponding to the imaginary frequency at the transition state indicates that this vibration is essentially the characteristic H atom motion between the $O_{phenolic}$ and O_{OOH} atoms. Cartesian coordinates of the prereactive complexes and transition structures are given in Table S2 of the Supporting Information. Relative energies (including ZPE) and Gibbs free energies (including thermodynamic corrections), calculated at the M05-2X/6-311++G** level, are reported in Table 4.

Table 4. Energies (Including ZPE) and Gibbs Free Energies (Including TCE at 298 K), in kcal mol^{-1}, in the Phenolic H-Abstractions by $^{\bullet}$OOH Radicals in Water

path	ΔE_1	$\Delta E^{\ddagger}$	ΔE	ΔG_1	$\Delta G^{\ddagger}$	ΔG
C-3A	−0.84	12.45	1.97	6.53	20.25	−0.73
C-5A	−1.44	12.12	1.36	6.24	19.77	−1.27
C-4B	−1.28	9.67	−4.47	6.04	17.96	−7.14

Values of the rate coefficients for phenolic hydrogen abstractions are reported in Table 5. Tunneling corrections (k) have been estimated by using the prereactant complexes as reactants, since these are collisionally stabilized in solution, and are also reported in Table 5. This is especially important for HAT channels, which are the ones susceptible to quantum tunneling. In all cases, tunneling is very large, in agreement with

Table 5. Imaginary Frequencies (ν^*, cm^{-1}), Tunneling Coefficients (κ), and Thermal TST Rate Constants (k, M^{-1} s^{-1}), at 298 K, in the H-Abstraction by $^{\bullet}$OOH Radicals in Water

path	ν^*	κ	k^{HAT}	Γ (%)
C-3A	−2788	2.07×10^3	9.10×10^2	~0.6
C-5A	−2915	3.50×10^3	3.40×10^3	~2.4
C-4B	−3092	6.70×10^3	1.38×10^5	~97.2

the calculated large imaginary frequencies, an indication of high and narrow barriers. This is typical of a relatively large O---H---O barrier due to hydrogen bonds present in the entrance and exit complexes.[80] Since rates are much slower than diffusion, it is not necessary to make a diffusion correction, as in the case of reaction with $^{\bullet}$OH. The observed high selectivity indicates that the formed radicals are intermediates in the formation of the final products. Again, the resveratrol C-4B hydroxyl group is the most reactive site because of the resonance effects.

As calculated from data in Table 5, the total rate constant in the HAT H-abstraction channels is approximately equal to 1.42×10^5 M^{-1} s^{-1} at 298 K, much lower than the diffusion limit (1.86×10^9 M^{-1} s^{-1}).

The SEPT mechanism has also been investigated. The proposed two-step SEPT mechanism for *trans*-resveratrol oxidation by $^{\bullet}$OOH radicals is analoguous to the one for the $^{\bullet}$OH SEPT mechanism and is depicted in Scheme 2. The diffusion limit rate constant, k_D, has been calculated using eq 5. As in the case of the $^{\bullet}$OH radical, ΔE^{SET} has been calculated as the nonadiabatic energy difference between reactants and vertical products, i.e., radical cation RV$^{\bullet+}$ and $^{\bullet}$OOH$^-$ at the neutral RV and $^{\bullet}$OOH geometries, respectively. The calculated Gibbs free energy of activation ($\Delta G^{\ddagger}$) in the SEPT mechanism is 18.14 kcal/mol, which is lower than the phenolic C-3A and C-5A H-abstraction pathways. Thus, the rate constant for this mechanism is not negligible when compared to the one for phenolic hydrogen abstraction, and it cannot be ruled out. The calculated SEPT reaction rate constant is 7.65 M^{-1} s^{-1} at 298 K, much lower than the HAT one. In this case, the HAT H-abstraction pathway is probably favored over the SEPT process.

As in the case of the $^{\bullet}$OH radical, another process may also occur, which leads to $^{\bullet}$OOH radical addition to either the >C═C< moiety (at positions Cα and Cβ) or to the aromatic rings.

The thermochemical feasibility of the $^{\bullet}$OOH-addition pathways was investigated first, since it determines the viability of any chemical process. Relative energies (ΔE) and Gibbs free energies of reaction (ΔG) for all addition channels are reported in Table 6.

These results are very different than the ones obtained with the $^{\bullet}$OH radical; as can be seen from Table 6, all $^{\bullet}$OOH-addition channels are endergonic. Therefore, they will not be considered in this work as, even if they took place at a significant rate, they would be reversible, and therefore, the formed products would not be observed. Moreover, since the reverse reaction is a unimolecular process, the rate constants of the direct and reverse reactions are not directly comparable. The behavior of such a system would strongly depend on reaction conditions, particularly on the reacting species concentrations. Under experimental and physiological conditions, such concentrations are far below the standard state 1 M, which means that the reverse process is largely favored, and consequently, pseudo-first-order equilibrium constants should necessarily be used. This methodology was recently successfully employed to explain similar cases in atmospheric chemistry.[81] It should be noticed that addition channels might, in principle, still be significant if their products rapidly react further and if no fast parallel reactions occur. This would be particularly important if these later stages were sufficiently exergonic to provide a driving force, and if their reaction barriers were low. This is not the case here.

The difference in reactivity between $^{\bullet}$OH and $^{\bullet}$OOH radicals can be directly related to the electron-accepting character of the

dx.doi.org/10.1021/jo3002134 | J. Org. Chem. 2012, 77, 3868−3877

Scheme 2. SET Mechanism for *trans*-Resveratrol Oxidation by •OOH Radicals

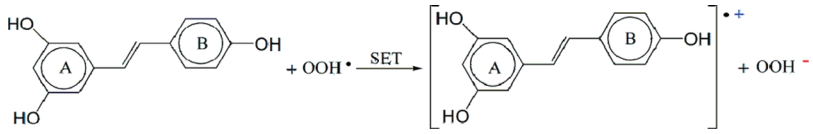

Table 6. Relative Reaction Energies (Including ZPE) and Gibbs Free Energies (Including TCE at 298 K), in kcal mol^{-1}, in *trans*-Resveratrol + •OOH Pathways in Water

•OOH-addition path	ΔE	ΔG
Cα	−8.58	0.49
Cβ	−7.88	1.31
C1A	13.62	22.43
C2A	1.90	11.09
C3A	8.47	17.30
C4A	−0.30	8.53
C5A	8.18	16.78
C6A	0.95	10.22
C1B	9.90	18.98
C2B	3.94	12.75
C3B	7.20	16.40
C4B	−0.16	8.88
C5B	7.74	16.77
C6B	1.68	11.03

reacting radical, which is in turn related to the much stronger O−H bond energy in water, as compared with the one in hydrogen peroxide.

Since the •OOH scavenging activity of *trans*-resveratrol takes place almost exclusively by HAT H-abstraction from site 4B, only one product of reaction is expected to be formed to a significant extent.

The overall rate coefficient for the *trans*-resveratrol + •OOH reaction in an aqueous environment is equal to the phenolic HAT H-abstraction rate, 1.42×10^5 M^{-1} s^{-1}, at 298 K. This reaction rate is very fast, and taking into account the relative concentrations of •OH and •OOH radicals in tissues, it can be safely concluded that the reaction rate of resveratrol with •OOH is even faster than the one with OH radicals. It is important then to compare the rate constant of •OOH with resveratrol with, for example, the rate constant of the •OOH damage to unsaturated fatty acids that occurs at much slower rate constants[50] $k = 1.18-3.05 \times 10^3$ M^{-1} s^{-1}, i.e., 2 orders of magnitude slower. Thus, we can conclude that *trans*-resveratrol prevents cellular damage by directly trapping •OOH radicals.

CONCLUSIONS

In this work, we have carried out a systematic study of the reactivity of *trans*-resveratrol toward hydroxyl (•OH) and hydroperoxyl (•OOH) radicals in aqueous simulated media using density functional quantum chemistry and computational kinetics methods. All possible mechanisms have been considered: hydrogen atom transfer (HAT), proton-coupled electron transfer (PCET), sequential electron proton transfer (SEPT), and radical adduct formation (RAF). Rate constants have been calculated using conventional transition state theory in conjunction with the Collins−Kimball theory. Branching ratios for the different paths contributing to the overall reaction, at 298 K, are reported.

For the overall reactivity of *trans*-resveratrol toward •OH radicals in water at physiological pH, several mechanisms contribute to the overall rate constant. Our results indicate that almost all channels are diffusion-controlled, thus, a mixture of all the possible products will be expected. The calculated overall diffusion-corrected rate constant for RV + •OH in aqueous solution is equal to 2.26×10^{10} M^{-1} s^{-1} at 298 K. The calculated branching ratios show that the OH scavenging activity of *trans*-resveratrol takes place predominantly by a RAF mechanism (∼ 61.9%). However, the rate constant of the SEPT reaction (7.95×10^9 M^{-1} s^{-1}) is larger than any individual RAF rate constant. In addition, it is interesting to point out that, because single electron transfer (SET) can occur when the reactants are at much larger distances than either in direct H-abstraction or •OH-addition mechanisms. Thus, in the RV + •OH reaction, in water at physiological pH, the main mechanism is proposed to be the sequential electron proton transfer (SEPT).

Regarding the reactivity of *trans*-resveratrol as an •OOH radical scavenger, we find that HAT H-abstractions from the phenolic groups are the only thermodynamically feasible reaction channels in water. The total rate coefficient is predicted to be 1.42×10^5 M^{-1} s^{-1}, smaller than the ones for reactions of *trans*-resveratrol with •OH radicals, but still very fast. Since the •OOH half-life time is several orders larger than the one of the •OH radical, these reactions should contribute significantly to *trans*-resveratrol oxidation in aqueous biological media. Thus, we can conclude that trans-resveratrol acts as a very efficient •OOH (and probably other structurally similar •OOR radicals) scavenger.

ASSOCIATED CONTENT

Supporting Information

Cartesian coordinates of all the RAF transition structures in the *trans*-resveratrol oxidation by •OH radicals in water (Table S1) and Cartesian coordinates of the H-abstraction prereactive complexes and transition structures in the *trans*-resveratrol oxidation by •OOH radicals in water (Table S2). This material is available free of charge via the Internet at http://pubs.acs.org.

AUTHOR INFORMATION

Corresponding Author

*E-mail: ciuga@xanum.uam.mx, nrusso@unical.it.

Notes

The authors declare no competing financial interest.

ACKNOWLEDGMENTS

This work is a result of the FONCICYT Mexico−EU 'RMAYS' network, Project No. 94666. We gratefully acknowledge the Laboratorio de Visualización y Cómputo Paralelo at Universidad Autónoma Metropolitana-Iztapalapa for computer time.

REFERENCES

(1) Fremont, L. *Life Sci.* **2000**, *66*, 663−673.
(2) Sanders, T. H.; McMichael, R. W.; Hendrix, K. W. *J. Agric. Food Chem.* **2000**, *48*, 1243−1246.

(3) Cai, Y. G.; Fang, J. G.; Ma, L. P.; Yang, L.; Liu, Z. L. *Biochem. Biophys. Acta* **2003**, *31*, 1637.
(4) Surh, Y. J.; Hurh, J. Y.; Lee, E.; Kong, G.; Lee, S. *Cancer Lett.* **1999**, *140*, 1.
(5) Soobrattee, M. A.; Neergheen, V. S.; Luximon-Ramma, A.; Aruoma, O. I.; Bahorun, T. *Mutat. Res.* **2005**, *579*, 200−213.
(6) Harman, D. *J. Am. Geriatr. Soc.* **1972**, *20*, 145−147.
(7) Corral-Debrinski, M.; Shoffner, J. M.; Lott, M. T.; Wallace, D. C. *Mutat. Res.* **1992**, *275*, 169−180.
(8) Judge, S.; Jang, Y. M.; Smith, A.; Hagen, T.; Leeuwenburgh, C. *FASEB J.* **2005**, *19*, 419−421.
(9) Mansouri, A.; Muller, F. L.; Liu, Y.; Ng, R.; Faulkner, J.; Hamilton, M.; Richardson, A.; Huang, T. T.; Epstein, C. J.; Van Remmen, H. *Mech. Ageing Dev.* **2006**, *127*, 298−306.
(10) Melov, S.; Shoffner, J. M.; Kaufman, A.; Wallace, D. C. *Nucleic Acids Res.* **1995**, *23*, 4122−4126.
(11) Schriner, S. E.; Linford, N. J.; Martin, G. M.; Treuting, P.; Ogburn, C. E.; Emond, M.; Coskun, P. E.; Ladiges, W.; Wolf, N.; Van Remmen, H.; Wallace, D. C.; Rabinovitch, P. S. *Science* **2005**, *308*, 1909−1911.
(12) Ungvari, Z. I.; Labinskyy, N.; Gupte, S. A.; Chander, P. N.; Edwards, J. G.; Csiszar, A. *Am. J. Physiol. Heart Circ. Physiol.* **2008**, *294*, H2121−H2128.
(13) Ungvari, Z. I.; Orosz, Z.; Labinskyy, N.; Rivera, A.; Xiangmin, Z.; Smith, K. E.; Csiszar, A. *Am. J. Physiol. Heart Circ. Physiol.* **2007**, *293*, H37−H47.
(14) Van Remmen, H.; Richardson, A. *Exp. Gerontol.* **2001**, *36*, 957−968.
(15) Labinskyy, N.; Mukhopadhyay, P.; Toth, J.; Szalai, G.; Veres, M.; Losonczy, G.; Pinto, J. T.; Pacher, P.; Ballabh, P.; Podlutsky, A.; Austad, S. N.; Csiszar, A.; Ungvari, Z. *Am. J. Physiol. Heart Circ. Physiol.* **2009**, *296*, H946−H956.
(16) Pearson, K. J.; Baur, J. A.; Lewis, K. N.; Peshkin, L.; Price, N. L.; Labinskyy, N.; Swindell, W. R.; Kamara, D.; Minor, R. K.; Perez, E.; Jamieson, H. A.; Zhang, Y.; Dunn, S. R.; Sharma, K.; Pleshko, N.; Woollett, L. A.; Csiszar, A.; Ikeno, Y.; Le Couteur, D.; Elliott, P. J.; Becker, K. G.; Navas, P.; Ingram, D. K.; Wolf, N. S.; Ungvari, Z.; Sinclair, D. A.; de Cabo, R. *Cell Metab.* **2008**, *8*, 157−168.
(17) Sharma, S.; Anjaneyulu, M.; Kulkarni, S. K.; Chopra, K. *Pharmacology* **2006**, *76*, 69−75.
(18) Su, H. C.; Hung, L. M.; Chen, J. K. *Am. J. Physiol. Endocrinol Metab.* **2006**, *290*, E1339−E1346.
(19) Thirunavukkarasu, M.; Penumathsa, S. V.; Koneru, S.; Juhasz, B.; Zhan, L.; Otani, H.; Bagchi, D.; Das, D. K.; Maulik, N. *Free Radical Biol. Med.* **2007**, *43*, 720−729.
(20) Zang, M.; Xu, S.; Maitland-Toolan, K. A.; Zuccollo, A.; Hou, X.; Jiang, B.; Wierzbicki, M.; Verbeuren, T. J.; Cohen, R. A. *Diabetes* **2006**, *55*, 2180−2191.
(21) de Lorgeril, M.; Salen, P.; Martin, J. L.; Monjaud, I.; Delaye, J.; Mamelle, N. *Circulation* **1999**, *99*, 779−785.
(22) Keys, A.; Menotti, A.; Karvonen, M. J.; Aravanis, C.; Blackburn, H.; Buzina, R.; Djordjevic, B. S.; Dontas, A. S.; Fidanza, F.; Keys, M. H.; Kromhout, D.; Nedeljkovic, S.; Punsar, S.; Seccareccia, F.; Toshima, H. *Am. J. Epidemiol.* **1986**, *124*, 903−915.
(23) (a) Surh, Y. J.; Hurh, Y. J.; Kang, J. Y.; Lee, E.; Kong, G.; Lee, S. J. *Cancer Lett.* **1999**, *140*, 1−10. (b) Asensi, M.; Medina, I.; Ortega, A.; Carretero, J.; Baño, M. C.; Obrador, E.; Estrela, J. M. *Free Radical Biol. Med.* **2002**, *33*, 387−398. (c) Hsieh, T. C.; Wu, J. M. *Exp. Cell Res.* **1999**, *249*, 109−115. (d) Soleas, G. J.; Grass, L.; Josephy, P. D.; Goldberg, D. M.; Diamandis, E. P. *Clin. Biochem.* **2002**, *35*, 119−124. (e) Hsieh, T. C.; Burfeind, P.; Laud, K.; Backer, J. M.; Traganos, F.; Darzynkiewicz, Z.; Wu, J. M. *Int. J. Oncol.* **1999**, *15*, 245−252.
(24) Casper, R. F.; Quesne, M.; Rogers, I. M.; Shirota, T.; Jolivet, A.; Milgrom, E.; Savouret, J. F. *Mol. Pharmacol.* **1999**, *56*, 784−790.
(25) Yagi, K., Ed. *Lipid Peroxides in Biology and Medicine*; Academic Press: New York, 1982.
(26) Dargel, R. *Exp. Toxicol. Pathol.* **1992**, *44*, 169.
(27) Anbar, N.; Neta, P. *Int. J. Appl. Radiat. Isot.* **1967**, *18*, 493−523.
(28) Dorfman, L. M.; Adams, G. E. *National Standard Reference Data System*; National Bureau of Standards 46, Washington, DC, 1973.
(29) Bielski, B. H.; Gebieki, J. M. In *Free Radicals in Biology*; Pryor, W. A., Ed.; Academic Press: New York, 1977; Vol. 3, pp 2−48,.
(30) Cohen, G. *Photochem. Photobiol.* **1978**, *28*, 669−675.
(31) Brawn, K.; Fridovich, I. *Arch. Biochem. Biophys.* **1981**, *206*, 414−419.
(32) Richmond, R.; Halliwell, B.; Chauhan, J.; Darbre, A. *Anal. Biochem.* **1981**, *118*, 328−335.
(33) Land, E. J.; Ebert, M. *Trans. Faraday Soc.* **1967**, *63*, 1181−1190.
(34) Ingelman-Sundberg, M.; Ekstrom, G. *Biochem. Biophys. Res. Commun.* **1982**, *106*, 625−631.
(35) Wang, M.; Li, J.; Rangarajan, M.; Shao, Y.; Lavoie, E. J.; Huang, T. C.; Ho, C. T. *J. Agric. Food Chem.* **1998**, *46*, 4869−4873.
(36) Stivala, L. A.; Savio, M.; Carafoli, F.; Perucca, P.; Bianchi, L.; Maga, G.; Forti, L.; Pagnoni, U. M.; Albini, A.; Prosperi, E.; Vannini, V. *J. Biol. Chem.* **2001**, *276*, 22586.
(37) Sandra, S.; Ortwin, B. *Phys. Chem. Chem. Phys.* **2002**, *4*, 757.
(38) Ortwin, B.; Sandra, S.; Helmut, S. *Free Radical Res.* **2002**, *36*, 76.
(39) Petralia, S.; Spatafora, C.; Tringali, C.; Foti, M. C.; Sortino, S. *New J. Chem.* **2004**, *28*, 1484.
(40) Queiroz, A. N.; Bruno, A. Q.; Moraes, M. W.; Borges, R. S. *Eur. J. Med. Chem.* **2008**, *30*, 1.
(41) Leopoldini, M.; Marino, T.; Russo, N.; Toscano, M. *J. Phys. Chem. A* **2004**, *108*, 4916−4922.
(42) Leopoldini, M.; Russo, N.; Toscano, M. *Food Chem.* **2011**, *125*, 288−306.
(43) Caruso, F.; Tanski, J.; Villagas-Estrada, A.; Rossi, M. *J. Agric. Food Chem.* **2004**, *52*, 7279.
(44) Cao, H.; Pan, X.; Li, C.; Zhou, C.; Deng, F.; Li, T. *Bioorg. Med. Chem. Lett.* **2003**, *13*, 1869.
(45) Leopoldini, M.; Russo, N.; Toscano, M. *J. Agric. Food Chem.* **2006**, *54*, 3078−3085.
(46) Pryor, W. A. *Free Radical Biol. Med.* **1988**, *4*, 219.
(47) Draganic, I. G.; Draganic, Z. D. *The Radiation Chemistry of Water*;Academic Press: New York, 1971.
(48) Pryor, W. A. *Annu. Rev. Physiol.* **1986**, *48*, 657.
(49) Marnett, L. *J. Carcinogenesis* **1987**, *8*, 1365.
(50) de Grey, A. D. N. *J. DNA Cell Biol.* **2002**, *21*, 251.
(51) Gaussian 09, Revision A.02: Frisch, M. J.; Trucks, G. W.; Schlegel, H. B.; Scuseria, G. E.; Robb, M. A.; Cheeseman, J. R.; Scalmani, G.; Barone, V.; Mennucci, B.; Petersson, G. A.; Nakatsuji, H.; Caricato, M.; Li, X.; Hratchian, H. P.; Izmaylov, A. F.; Bloino, J.; Zheng, G.; Sonnenberg, J. L.; Hada, M.; Ehara, M.; Toyota, K.; Fukuda, R.; Hasegawa, J.; Ishida, M.; Nakajima, T.; Honda, Y.; Kitao, O.; Nakai, H.; Vreven, T.; Montgomery, J. A., Jr.; Peralta, J. E.; Ogliaro, F.; Bearpark, M.; Heyd, J. J.; Brothers, E.; Kudin, K. N.; Staroverov, V. N.; Kobayashi, R.; Normand, J.; Raghavachari, K.; Rendell, A.; Burant, J. C.; Iyengar, S. S.; Tomasi, J.; Cossi, M.; Rega, N.; Millam, J. M.; Klene, M.; Knox, J. E.; Cross, J. B.; Bakken, V.; Adamo, C.; Jaramillo, J.; Gomperts, R.; Stratmann, R. E.; Yazyev, O.; Austin, A. J.; Cammi, R.; Pomelli, C.; Ochterski, J. W.; Martin, R. L.; Morokuma, K.; Zakrzewski, V. G.; Voth, G. A.; Salvador, P.; Dannenberg, J. J.; Dapprich, S.; Daniels, A. D.; Farkas, O.; Foresman, J. B.; Ortiz, J. V.; Cioslowski, J.; Fox, D. J. Gaussian, Inc., Wallingford CT, 2009.
(52) Zhao, Y.; Schultz, N. E.; Truhlar, D. G. *J. Chem. Theory Comput.* **2006**, *2*, 364.
(53) (a) Zavala-Oseguera, C.; Alvarez-Idaboy, J. R.; Merino, G.; Galano, A. *J. Phys. Chem. A* **2009**, *113*, 13913. (b) Velez, E.; Quijano, J.; Notario, R.; Pabón, E.; Murillo, J.; Leal, J.; Zapata, E.; Alarcón, G. *J. Phys. Org. Chem.* **2009**, *22*, 971. (c) Galano, A.; Alvarez- Idaboy, J. R. *Org. Lett.* **2009**, *11*, 5114. (d) Perez-Gonzalez, A.; Galano, A. *J. Phys. Chem. B* **2011**, *115*, 1306. (e) Leon-Carmona, J. R.; Galano, A. *J. Phys. Chem. B* **2011**, *115*, 4538. (f) Furuncuoglu, T.; Ugur, I.; Degirmenci, I.; Aviyente, V. *Macromolecules* **2010**, *43*, 1823. (g) Iuga, C.; Alvarez-Idaboy, J. R.; Vivier-Bunge, A. *J. Phys. Chem. A* **2011**, *115*, 5138. (h) Leon-Carmona, J. R.; Galano, A. *J. Phys. Chem. B* **2011**, *115*,

15430. (i) Perez- Gonzalez, A.; Galano, A. *J. Phys. Chem. B* **2011**, *115*, 10375.
(54) (a) Alvarez-Idaboy, J. R.; Mora-Diez, N.; Vivier-Bunge, A. *J. Am. Chem. Soc.* **2000**, *122*, 3715. (b) Alvarez-Idaboy, J. R.; Mora-Diez, N.; Boyd, R. J.; Vivier-Bunge, A. *J. Am. Chem. Soc.* **2001**, *123*, 2018. (c) Uc, V. H.; Alvarez-Idaboy, J. R.; Galano, A.; Vivier- Bunge, A. *J. Phys. Chem. A.* **2006**, *110*, 10155. (d) Iuga, C.; Alvarez-Idaboy, J. R.; Vivier-Bunge, A. *Theor. Chem. Acc.* **2011**, *129*, 209. (e) Iuga, C.; Alvarez-Idaboy, J. R.; Reyes, L.; Vivier-Bunge, A. *J. Phys. Chem. Lett.* **2010**, *1*, 3112.
(55) Marenich, A. V.; Cramer, C. J.; Truhlar, D. G. J. *Phys. Chem. B* **2009**, *113*, 6378.
(56) Okuno, Y. *Chem.—Eur. J.* **1997**, *3*, 212.
(57) Benson, S. W. *The Foundations of Chemical Kinetics*; Krieger: Malabar, FL, 1982.
(58) Ardura, D.; Lopez, R.; Sordo, T. L. *J. Phys. Chem. B* **2005**, *109*, 23618.
(59) Eyring, H. *J. Chem. Phys.* **1935**, *3*, 107.
(60) Evans, M. G.; Polanyi, M. *Trans. Faraday Soc.* **1935**, *31*, 875.
(61) Truhlar, D. G.; Hase, W. L.; Hynes, J. T. *J. Phys. Chem.* **1983**, *87*, 2264.
(62) Duncan, W. T.; Bell, R. L.; Truong, T. N. *J. Comput. Chem.* **1998**, *19*, 1039.
(63) Zhang, S.; Truong, T. N. VKLab version 1.0, University of Utah, 2001.
(64) Truhlar, D. G.; Kuppermann, A. *J. Am. Chem. Soc.* **1971**, *93*, 1840−1851.
(65) Eckart, C. *Phys. Rev.* **1930**, *35*, 1303.
(66) Marcus, R. A. *Annu. Rev. Phys. Chem.* **1964**, *15*, 155.
(67) Marcus, R. A. *Rev. Mod. Phys.* **1993**, *65*, 599.
(68) Marcus, R. A. *Pure Appl. Chem.* **1997**, *69*, 13.
(69) Nelsen, S. F.; Blackstock, S. C.; Kim, Y. *J. Am. Chem. Soc.* **1987**, *109*, 677.
(70) Nelsen, S. F.; Weaver, M. N.; Luo, Y.; Pladziewicz, J. R.; Ausman, L. K.; Jentzsch, T. L.; O'Knek, J. J. *J. Phys. Chem. A* **2006**, *110*, 11665.
(71) Collins, F. C.; Kimball, G. E. *J. Colloid Sci.* **1949**, *4*, 425.
(72) Smoluchowski, M. Z. *Phys. Chem.* **1917**, *92*, 129.
(73) Truhlar, D. G. *J. Chem. Educ.* **1985**, *62*, 104.
(74) (a) Einstein, A. *Ann. Phys. (Leipzig)* **1905**, *17*, 549. (b) Stokes, G. G. *Mathematical and Physical Papers*; Cambridge University Press: Cambridge, 1903; Vol. 3 (esp Section IV, p 55).
(75) Chiodo, S. G.; Leopoldini, M.; Russo, N.; Toscano, M. *Phys. Chem. Chem. Phys.* **2010**, *12*, 7662−7670.
(76) Iuga, C.; Alvarez-Idaboy, J. R.; Vivier-Bunge, A. *J. Phys. Chem. B* **2011**, *115*, 12234−12246.
(77) See, for example: (a) Galano, A.; Francisco-Marquez, M.; Alvarez-Idaboy, J. R. *Phys. Chem. Chem. Phys.* **2011**, *13*, 11199. (b) Galano, A.; Francisco-Márquez, M.; Alvarez-Idaboy, J. R. *J. Phys. Chem. B* **2011**, *115*, 8590. (c) Galano, A.; Alvarez-Idaboy, J. R. *RSC Advances* **2011**, *1*, 1763. (d) Galano, A. *Phys. Chem. Chem. Phys.* **2011**, *13*, 7147.
(78) Butler Ricks, A.; Solomon, G. C.; Colvin, M. T.; Scott, A. M.; Chen, K.; Ratner, M. A.; Wasielewski, M. R. *J. Am. Chem. Soc.* **2010**, *132* (43), 15427.
(79) Friedman, M. *J. Agric. Food Chem.* **1997**, *45*, 1523.
(80) Galano, A.; Alvarez-Idaboy, J. R.; Ruiz-Santoyo, M. E.; Vivier-Bunge, A. *J. Phys. Chem. A* **2002**, *106*, 9520.
(81) (a) Uc, V. H.; Alvarez-Idaboy, J. R.; Galano, A.; Vivier-Bunge, A. *J. Phys. Chem. A* **2008**, *112*, 7608. (b) Galano, A.; Narciso-Lopez, M.; Francisco-Marquez, M. *J. Phys. Chem. A* **2010**, *114*, 5796. (c) Iuga, C.; Alvarez-Idaboy, J. R.; Reyes, L.; Vivier-Bunge, A. *J. Phys. Chem. Lett.* **2010**, *1*, 3112.